Eleventh International Conference on CFD in the Minerals and Process Industries
CSIRO, Melbourne, Australia
7-9 December 2015

FLEXIBLE PIPE EROSION MODELLING

Chong Y. WONG[1*], Christopher B. SOLNORDAL[1] and Henri MORAND[2]

[1] CSIRO Minerals Resources Flagship, Clayton, Victoria 3169, AUSTRALIA
[2] Technip, Perth, Western Australia 6005, AUSTRALIA
*Corresponding author, E-mail address: chong.wong@csiro.au

ABSTRACT

Flexible pipes are commonly used by Floating Production Storage Offloading (FPSO) vessels to transport produced oil and gas fluids in subsea pipe network installations in place of rigid pipework. The innermost layer of the pipe (interlocked carcass) is in direct contact with the produced fluids which may also transport sand particles causing inner surface erosion over time. The rate of erosion on a material's surface is approximately proportional to the square of the particle impact velocity and particles in gas flows travel at a greater relative velocity than liquid flows. Therefore, the use of flexible pipes in gas dominant fields will be more prone to sand erosion than those in liquid dominant fields. A review of the literature revealed numerous experimental and modelling papers on smooth bore rigid bent pipe, but very limited information is available for roughbore flexible pipes. The contribution of the current paper is to propose a new model based on DNV-RP-O501 to analytically predict the erosion rate of the detailed internal carcass of a roughbore flexible pipe. The new model, benchmarked against literature data and CFD simulations, accounts for variations in erosion rate with particle impact angle to allow more detailed erosion profiling of the internal carcass. The work will provide a platform for further development, testing and calibration which might ultimately enable flexible pipe designers to improve solid particle erosion estimations, specifically in dry gas fields.

NOMENCLATURE

C_1	Model geometry factor, 2.5 [-]
C_{unit}	Unit conversion factor m/s to mm/year
A_{pipe}	Pipe internal cross-sectional area [m^2]
d	Particle diameter [m]
D	Pipe diameter [m]
d_{50}	Particle diameter at 50th percentile [m]
e	specific erosion rate (kg/s of material removed / kg/s of impacting erodent) [-]
E_L	Lineal erosion rate [mm/year]
E_W	Erosion rate [kg of material removed per sec]
$F(\alpha)$	Mathematical function of particle impact angle that typically includes additional empirical constants, $0<F(\alpha)\leq 1$ [-]
G	Size correction function in DNV RP O501
K	Material scaling coefficient [$(m/s)^{-n}$]
L	Equivalent stagnation length [inches]
L_0	1.18 [inches]
m	Gradient value of position in x-y plane [-]
$\dot{m}_p$	Mass of particles arriving at target per second [kg/s]
n	Velocity exponent [-]
R_c	Radius of bend [m]
V	Velocity [m/s]
x, y	Symbols defined in 3a
α	Particle impact angle [degrees]
ρ	Density [kg m^{-3}]
μ	Dynamic viscosity [kg m^{-1} s^{-1}]
θ	Angular location from start of bend [degrees]

Subscript

p	Particle
f	Fluid
SG	Superficial gas or bulk gas velocity
t	Target material

INTRODUCTION

Rough bore flexible pipes are commonly used to transport produced oil and gas fluids in subsea pipe network installations in place of rigid pipework. They are especially suited for use with Floating Production Storage Offloading (FPSO) vessels due to their ability to account for a vessel's dynamic motion. These pipes are constructed of multiple layers of material with each layer performing a specific function. The innermost layer of the pipe is known as the interlocked carcass and is in direct contact with the produced fluids. The produced fluids may also transport sand particles which over time can lead to solid particle erosion on the inner surfaces of these carcasses (Togersen, Lejon *et al.*, 2006), eventually resulting in pipe damage.

It is known that the rate of erosion on a material's surface is generally proportional to the square of the particle impact velocity (Finnie, 1960). Therefore, the use of flexible pipes in gas dominant fields where the particle velocities are higher will be more prone to sand erosion than those in liquid dominant fields. As such, there is a need to increase the understanding in the design for erosion prediction of flexible (unbonded) pipelines in gas dominant fields. This paper has identified a few erosion methodologies related to curved smooth and curved roughbore pipes and proposes an improved model based on an existing erosion model for curved roughbore pipes.

The literature covering erosion by sand particles in flow around bends of smooth pipes is numerous and there are several erosion models that predict the location and severity of the maximum erosion position around a bend. Most of these models take the form proposed by Finnie (Finnie, 1960):

$$e = \frac{E_W}{\dot{m}_p} = KV_p^n F(\alpha) \quad (1)$$

Depending on the form of $F(\alpha)$, the model may account for material surface cutting when particles approach at low impact angles and at higher angles, material removal by deformation due to cratering leading to lip formation and material ejection from the lip edges. The advantage of this model is that it decouples the fluid mechanics from the erodent-target material interaction. The model shows that specific erosion rate is largely influenced by the particle impact velocity and the particle impact angle. The scaling coefficient, K, is also required to account for material dependent effects, and this is determined empirically. Care must be taken to associate a particular experimental condition with the measured erosion rate. For example, (Ruff, 1986) highlighted the large scatter in inter-laboratory experimental results of erosion tests for the same experimental conditions. His study found that small changes in the reported particle velocity, nozzle-material distance and nozzle diameter may lead to large changes in the erosion rate.

A thorough search of the related literature on rough bore flexible pipe erosion methodology only turned up one source (Kvernvold and Nokleberg, 1989) which reconfigured their smooth pipe erosion prediction for rough bore flexible pipes. Remaining literature search related to erosion predictions or experiments in smooth bore pipe bends. Most of the smooth bore pipe equations contained limited parameters to describe the complexities inherent in erosion prediction. Of these, (Bikbaev, Maksimenko *et al.*, 1973), (Bourgoyne, 1989), (DNV, 2007), (El-Behery, Hamed *et al.*, 2010), (McLaury, Wang *et al.*, 1997) and (McLaury, Shirazi *et al.*, 1999) present models that account for bend radius effects in smooth bore pipe bends.

From these models, the DNV model was found to be robust in estimating erosion rate as a function of particle impact angle. This relationship is important when considering erosion on the non-smooth regions of the internal carcass. As such, the DNV model is proposed as the backbone to develop a configuration-specific erosion model for rough bore flexible pipes. CFD was used to examine the fluid flow-fields and provide further understanding of the erosion hot-spots within the carcass.

MODEL DESCRIPTION

Prior to the development of this model, it is necessary to understand the sensitivity of each parameter in the Finnie equation as it relates to a roughbore model, and to examine reasons for the underlying assumptions.

Sensitivity Studies

Coefficients K and n

In Equation (1), the parameter K relates to material properties of both the eroding surface and the impacting material, while n is a velocity exponent. These parameters are usually determined empirically, and can have a significant impact on the overall results. Linear variations in K will have a linear effect on E, while small variations in n have a power law effect on E.

Parameter V_p

In the absence of available measurement data, the value of a characteristic particle velocity chosen is usually a bulk velocity term, V_{SG}. However, this does not reflect the actual velocity of the particle approaching the wall, V_p which is usually lower than V_f. Variations of V_p and V_f can be seen in Figure 1 (Jordan, 1998), where $\phi = L\rho_f / (d_p\rho_p)$, $Re = \rho_f V_f d_p / \mu_f$; for $\phi/Re < 0.153$. Particles will not impact walls when ϕ/Re is greater than this value.

The family of curves in Figure 1 are based on Jordan's reduced-order simplification of the Tulsa E/CRC model (Jordan, 1998). In most industrial cases (for high Stokes number flows), where velocities are high and particles moderately sized, V_p/V_f is not less than 0.9. In other words, for large particles in low density flows, expect V_p to be over-predicted by up to 10%. For smaller particles in high density flows, e.g. fines, this over-prediction can be more than 50%.

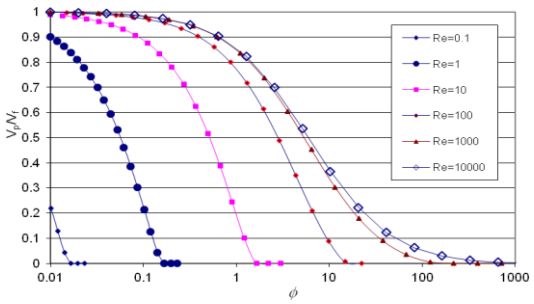

Figure 1: V_P/V_F versus ϕ derived from Jordan's reduced-order model (Jordan, 1998).

Function F(α)

Figure 2 compares the variation of $F(\alpha)$ of two typical shapes of erosion curves for ductile metals (Menguturk and Sverdrup, 1979) and (DNV 2007). In the range of interest where erosion is greatest in a curved flexible pipe, especially around $\alpha = 20°$ and $\alpha = 40°$, $F(\alpha) \geq 0.9$. Within this range of particle impact angles, the relative difference in $F(\alpha)$ values between these two profiles is about 30%.

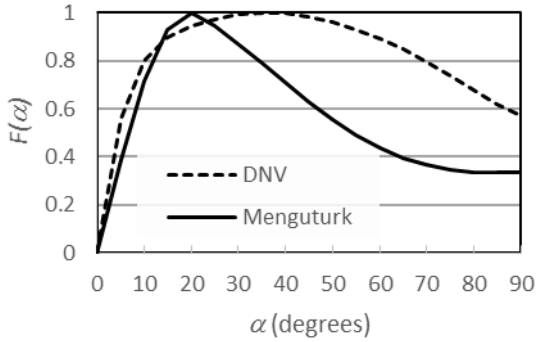

Figure 2: Comparing *F(a)* curves for ductile metals.

Presence of Irregularities on the carcass

It is thought that the presence of irregularities on the rough bore flexible pipe carcass surface may pose some erosion risk. (Kvernvold and Nokleberg, 1989) attempted to model these irregularities as triangular indentations on the smooth surface. That is, irregularities are defined here as the material excursions in the radial direction.

Their simulations suggest that maximum erosion on these irregularities may be up to an order of magnitude higher than the erosion on the smooth part of the carcass. However, this risk has not been previously quantified for

actual profiles using the carcass detail and accurately accounting for particle impact velocity. This paper improves the technique by accounting for specific carcass detail and particle impact velocity (via Jordan's reduced order modification to estimate V_p).

Model Development

The purpose of the model is to provide a method of estimating lineal erosion rate, E_L, in a rough surface pipe bend. The development of the model is outlined in the following sections. Initially, the assumptions are presented followed by the approach to develop an equation for E_L.

Model Assumptions

The following assumptions are made when applying the new model to predict erosion on the steel carcass:

1. Particles are uniformly distributed as they enter the flexible pipe bend.
2. Flow velocity distribution is modelled as a plug flow, so the axial flow velocity in any location of the pipe cross-section is the same.
3. Particle velocity is calculated based on Jordan's (1998) (Jordan, 1998) reduced-order simplification of Tulsa's ECRC model (Shirazi et al, 1995a) (Shirazi, McLaury *et al.*, 1995). This is the current model that accounts for the deceleration of a particle as it approaches the wall through a stagnation layer encountered in a pipe bend. Other models that do not account for this deceleration in particle velocity will over-predict the erosion rate in their calculations.
4. Effect of secondary vortices, commonly occurring in bend flows, is neglected since axial velocity component is more dominant than the radial velocity component in most engineering flows.
5. Particle diameter based on d_{50} is used. Particle size distribution is not considered.
6. Dilute concentration of particles is assumed, implying that particle-particle interaction is negligible.
7. Coefficients used in the model are based on the DNV-RP-O501 model which have been calibrated with specific experiments and are not suggested for general use, but serve as a qualitative guide only. Physical experiments are required to determine these new coefficients when a target material or sand type changes. The coefficients in $F(\alpha)$ describe the shape of the target material and particle interaction for a ductile material tested by DNV. No further information is provided by DNV as to the source of these coefficients or the derivation of $F(\alpha)$. As such, validity ranges for this cannot be obtained. However, variations in $F(\alpha)$ will account for nominally 30% differences in the predicted erosion rate results. The material constant, K, is for generic steel grades and is expected to vary depending on the type of steel used (e.g. Stainless steel 316, 304 or Duplex 2205). Again, these values have to be determined empirically against a given sand type and flow regime (e.g. liquid or gas) for a more accurate level of erosion prediction. DNV suggests that for velocities less than 100 m/s, differences in erosion resistance are generally within 10-20%. The velocity exponent n is intrinsically related to K and generally varies between 1.6 and 2.3 for ductile materials.
8. Gravitational effects on the particles are neglected in this model. Thus the model does not account for the orientation of the entry flow. However, the entry flow has been reported elsewhere to be an important factor in determining the location of the maximum wear point (Deng et al, 2005).

Estimation of material-particle factors and coefficients

The material-particle factor (K) provides an indication of the relative importance of factors such as sand sharpness, material hardness (e.g. Brinell Hardness), material strength, etc. on the model. However, coefficients relating the analytical model to physical models are necessary. Unfortunately, these coefficients are not generic and have to be determined on a case-by-case basis. O'Flynn et al (2001) (O'Flynn, Bingley *et al.*, 2001) and Sundararajan et al (Sundararajan, 1983; Sundararajan, 1991; Sundararajan, 1995) have tried to relate standard material properties (e.g. material hardness, true uniform strain, toughness, mechanical energy density, etc.) with erosion rate and met with limited success. To date there is no one model that accounts for the complexity of erosion modelling. Thus, all the models in this review to some degree contain simplification of specific materials-sand interaction. For example, the DNV model assumes "steel" to be all types of steels, including mild steel, stainless steel, etc.

Estimation of particle impact velocity

As a particle enters a bend, it is assumed to slow down. The distance over which the particle decelerates from the bulk superficial fluid velocity, V_{SG}, to its impact velocity at the wall, V_p, is known as the equivalent stagnation length, L. Shirazi et al (1995) (Shirazi, McLaury *et al.*, 1995) calculated L for a two-dimensional right angle turn and formulated an equation (in inches for Equation 2 only) to approximate the stagnation length, where $D \geq 0.3085$ inches:

$$\frac{L}{L_0} = 1 - 1.27 \arctan\left(1.01 D^{-1.89}\right) + D^{0.129} \qquad (2)$$

To estimate particle impact velocity, we require 3 dimensionless groups, namely, V_p/V_f, Reynolds number ($Re = \rho_f V_f d_p / \mu_f$) and ϕ ($\phi = L\rho_f/(d_p\rho_p)$). The reduced order formula provided by (Jordan, 1998) is used here:

$$V_p = V_f \left(1 - 10.147\left(\frac{\phi}{\mathrm{Re}}\right) + 23.62\left(\frac{\phi}{\mathrm{Re}}\right)^2\right)\left(\frac{1}{1+\frac{\phi}{6}}\right) \qquad (3)$$

Construct simplified carcass geometry profile

We assume that the most affected eroded region will occur on the surface of the carcass in contact with the sand bearing fluid, especially on surfaces away from the deep crevices. We can therefore re-draw the actual carcass profile Figure 3b into the simplified repeating profile shown in Figure 3c. CFD simulations confirmed that this is a valid assumption as little or no sand impacts onto the inner crevice surfaces.

Estimate particle impact angle on smooth surface of carcass

Calculate the path taken by high Stokes number particles to the first point of impact on the extrados of the bend for a given bend radius and pipe diameter. This neglects gravitational effects, particle-focusing effects or particle deviations by the flow or turbulence effects. The impact angle on the extrados (α) is shown as Equation (4).

$$\alpha = 77.74\left(\frac{R_c}{D}\right)^{-0.4899} \qquad (4)$$

Equation (4) assumes particles travel in a straight line from the commencement of the intrados to the point of impact at the extrados.

Calculate impacting plug flow angle onto the extrados

The impacting plug flow angle, α, as the plug flow travels in a straight line from the straight section of the pipe to the extrados is calculated based on Equation (4). This concept is analogous to conducting a direct impact experiment over all the particle impact angles whereby all the particles from the pipe 'jet' impact onto a circular plate with diameter, d, at a given angle, α. At $\alpha = 90°$, the plate cross-section experiences particle impact from all the sand mass emerging from the pipe. This is similar to a direct impingement erosion test. At $\alpha = 0°$ and in a simplistic way, ignoring any flow separation effects, the plate cross-sectional surface does not experience any erosion. At any angle between this, the projected area exposed to the sand impacting the circular plate surface can be expressed as:

$$A_t = \frac{A_{pipe}}{\sin(\alpha)} \tag{5}$$

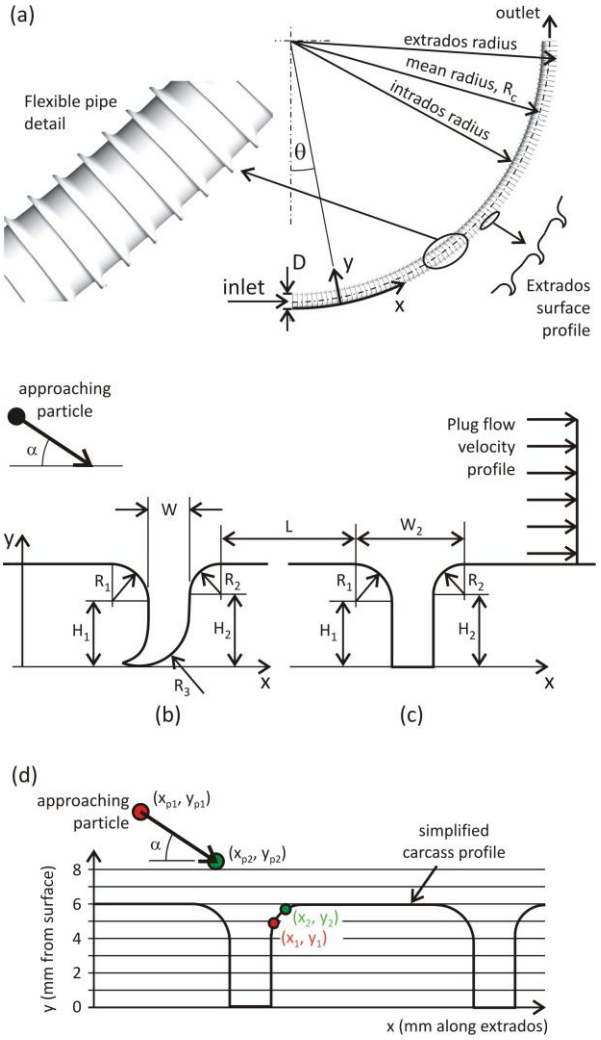

Figure 3: Details of the flexible pipe carcass. (a) Geometry with coordinates defined; (b) detail of actual extrados surface profile; (c) simplified extrados surface profile; (d) detail of coordinates.

Equation (5) accounts for the decrease in erosion rate on the global surface of the extrados with increasing curvature ratio. However, it does not account for the local variations of particle impact effects on the carcass profile.

To account for the local particle impact angles at the irregular surface, we do the following: For a given geometry and approaching particle impact to the wall defined by H_2 in Figure 3c and on the horizontal surface (on *x*-axis), plot (Figure 3c) the various local particle impact angles on the undulated surface (e.g. at (x_2, y_2)). First obtain the gradient value at (x_2, y_2) and (x_{p2}, y_{p2}) using the equations:

$$m_2(x_2, y_2) = \frac{(y_2 - y_1)}{(x_2 - x_1)} \tag{6}$$

$$m_{p2}(x_{p2}, y_{p2}) = \frac{(y_{p2} - y_{p1})}{(x_{p2} - x_{p1})} \tag{7}$$

where,

$$x_{p2} = x_{p1} + \frac{H_2\left(\cos\left(\frac{\alpha\pi}{180}\right)\right)}{2}, \quad y_{p2} = y_{p1} - \frac{H_2\left(\cos\left(\frac{\alpha\pi}{180}\right)\right)}{2}$$

Arbitrarily set x_{p1} and y_{p1} for a position above the carcass. Repeating this formula along the extrados over a local carcass element, and calculating the particle impact angle ($\alpha_{p,i}$) using following equation,

$$\alpha_{p,i}(x_2, y_2) = \frac{180}{\pi}\arctan\frac{(m_2 - m_{p2})}{(1 + m_2 m_{p2})} \tag{8}$$

we obtain the graph of local particle impact angle.

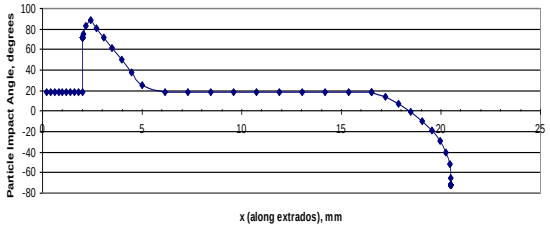

Figure 4: Graph showing local particle impact angle ($\alpha_{p,i}$) on carcass surface.

Next, individual F($\alpha_{p,i}$) values for each i^{th} surface location calculated for each local particle impact angle (e.g from DNV, Fig 7-2) is included into $F(\alpha)$. Re-writing the equation from DNV-RP-O501, we can calculate the erosion rate on the extrados of the flexible pipe bend using Equation (9):

$$E_{L,i} = \frac{\dot{m}_p K F(\alpha_{p,i}) \sin(\alpha) V_p^n}{\rho_t A_{pipe}} G C_1 C_{unit} \tag{9}$$

Particle velocity is calculated according to Jordan's (1998) reduced order method. Other parameters such as *n* and *K* are obtained from DNV (2007) directly. An example of the final result is shown in Figure 5.

Validation of new model with published experimental data

The erosion rate (mm/year) on a stainless steel carcass surface for conditions in a test case (test case 5-20 ppm-v/v) from (Kvernvold, 1990) using sharp 250 μm sand suspended in nitrogen gas flowing at bulk velocity of

18 m/s in a 50.8 mm ID (D) pipe with a bend centerline radius ratio (R_c/D) of 19.7 is shown in Figure 5. No mention of sand rate is provided thus a conservative figure of 20 ppm-v/v is used for the calculations. Using the $F(\alpha)$ data from DNV (2007) and for each carcass element, a peak erosion rate occurs on the transition between the curved surface and the smooth surface. The outline of the carcass is also shown as a physical reference. The regular surface is defined as the outline of the extrados surface for a smooth pipe while the irregular surface is any surface deviating outwards from the extrados surface.

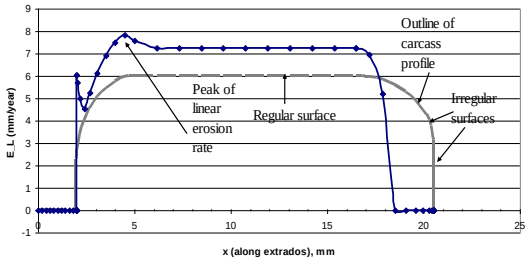

Figure 5: Erosion rate estimation on the carcass detail.

The new model, represented by Equation (9), is further validated with five other experimental datapoints covering the following test parameter variations with experimental details shown in Table 1.

Results of the new model are compared with other literature models that account for pipe curvature. These are shown in Figure 6. The new model predicts cases 2 to 5 within ±50% of the experimental data except for case #1 which is the low velocity and low curvature case. This is a reasonable result considering the complexity of erosion predictions and that experimental variations in K, n and $F(\alpha)$ determined for limited cases of materials and particles by DNV (2007) could reliably predict the erosion rates from different experiments conducted by different researchers (e.g. Bourgoyne, 1989).

Test #	Type of Bore	D [m]	R_c/D	Pipe Material	Sand vol. rate, Q_p [m^3/s] (ppm Vol)	d_{50} [μm]	V_{SG} [m/s]	Reference
1	Smooth	0.0508	1.5	Steel-1	1.7×10^{-5} (268)	500	32 (Air)	
2	Smooth	0.0508	1.5	Steel-1	5.3×10^{-5} (255)	500	103 (Air)	(Bourgoyne, 1989)
3	Smooth	0.0508	1.5	Steel-1	2.82×10^{-4} (1351)	500	103 (Air)	
4	Smooth	0.0508	4.5	Steel-2	1.52×10^{-4} (676)	500	111 (Air)	
5	Rough	0.0508	19.7	SS316 L	7.3×10^{-7} (20)	250	18 (N_2)	(Kvernvold, 1990)

Note: 1. Steel-1 is Seamless steel grade WPB; 2. Steel-2 is Cast grade WBC

Table 1: Summary of main physical test conditions for model comparisons.

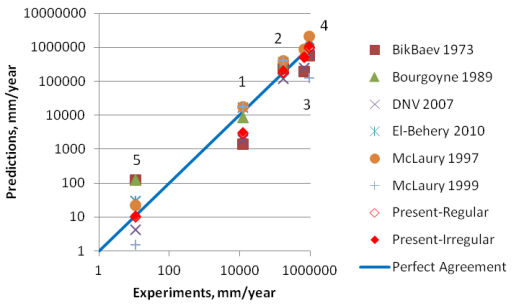

Figure 6: Validation of model with experimental data. Cases are labelled '1' to '5' adjacent to each data cluster.

CFD SIMULATION AND RESULTS

A CFD study for a 6" ID flexible pipe carcass passing through a bend angle of 90° (R_c/D = 18) was also performed to understand the flow paths and erosion effects of the particles within the flexible pipe. The flow conditions were natural gas (ρ_f = 77.3 kg/m^3, μ_f = 1.52 Pa s) at 100 bar-g and 110°C with 15 m/s bulk gas velocity. The sand used was quartz (2600 kg/m^3) with a mean size distribution of 55 μm and one standard deviation of 15 μm at a feed rate of 8.34×10^{-5} kg/s. Commercial CFD software ANSYS-CFX14 was used to calculate the dynamics of the fluid flow, the particle tracks and erosion predictions. The erosion model used was from (Elfeki and Tabakoff, 1987) using empirical constants presented in (ANSYS, 2012) for quartz on stainless steel. As these were not calibrated for specific conditions related to the flexible pipe, the simulations results should only be used as a guide.

It was observed that separated flow structures occurred on the intrados of the pipe most likely attributed to turbulent separated flow. This led in a narrowing of the bulk fluid flow through the non-separated regions of the pipe resulting in higher flow velocities in the vicinity of extrados of the bend. It was therefore not surprising that the maximum flow velocity and hence material removal rate were found on the extrados. In Figure 7, particle paths were concentrated towards the extrados of the bend, with the majority of particle impacts occurring on the forward-facing edge of each carcass rib giving the results presented in Figure 9.

In Figure 8, the erosion distribution was predicted to follow that of the particle path impacts, so that the highest erosion occurred on the extrados of the bend, on the forward-facing edge of each carcass rib. A region of reduced erosion was predicted to exist on the extrados surface, approximately along its intersection with the vertical centre-plane. The predicted erosion pattern was in good qualitative agreement with published erosion observations in flexible pipe bends (Togersen, Lejon *et al.*, 2006).

The location of maximum erosion was predicted to occur at an azimuthal angle of $\theta = 23.75°$ into the 90° bend (Figure 8). This location corresponded to the point at which the high velocity gas entering the bend first encounters the extrados of the bend.

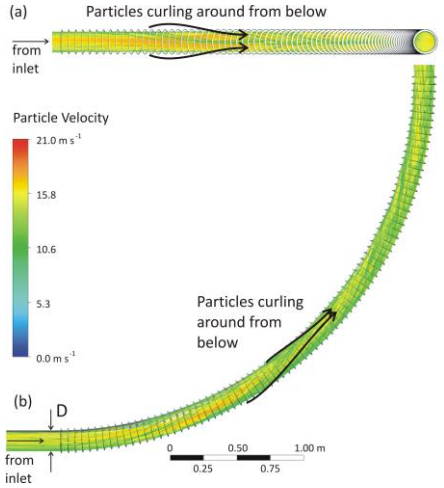

Figure 7: CFD of particle tracks through bend: (a) Plan view and (b) elevation view.

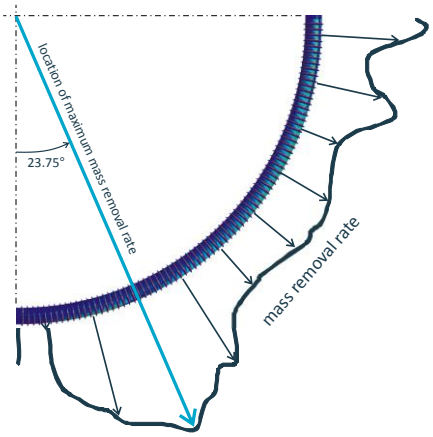

Figure 8: Mass removal rate shown diagrammatically around the flexible pipe bend, from CFD. Flow enters from lower left.

In Figure 9, the predicted maximum erosion rate is 0.028 mm/year for the conditions studied, while the nominal erosion rate on the regular smooth surface is 0.0004 mm/year, a difference of 700%. The results from the hand calculated model only predicts a difference of about 6%. One hypothesis for the higher than expected maximum erosion rate could be due to enhanced particle impacts there. The increased number of impacts is in turn postulated to be due to preferential clustering of particles and turbulence coupled with the complex separated flows above the crevices of each carcass segment.

Figure 10 shows the various hand calculations compared with results from the CFD simulations on the regular and irregular walls of the carcass. For regular wall predictions, some of the literature models (i.e. Bikbaev, El-Behery and McLaury-1997) over-predict the CFD results by greater than 2 orders of magnitude. However, DNV, Bourgoyne, McLaury-1999 and the present models provide predictions of about one order of magnitude to the CFD predictions for regular walls. For irregular wall predictions, the present model predicts within one order of magnitude to the CFD results. Therefore, in the absence of further physical erosion data, the new methodology will be at best an order of magnitude first guess.

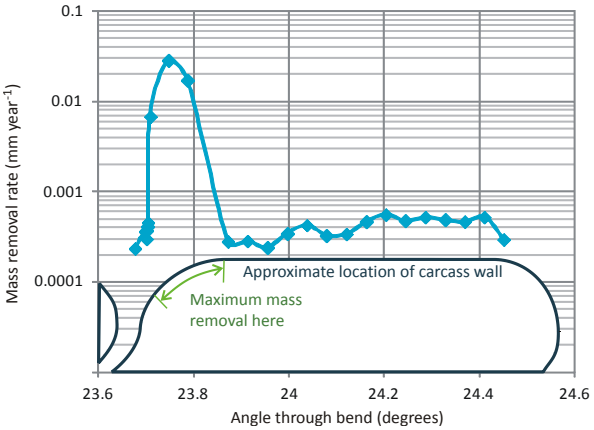

Figure 9: Mass removal rate at maximum erosion location (θ = 23.75° into bend), from CFD.

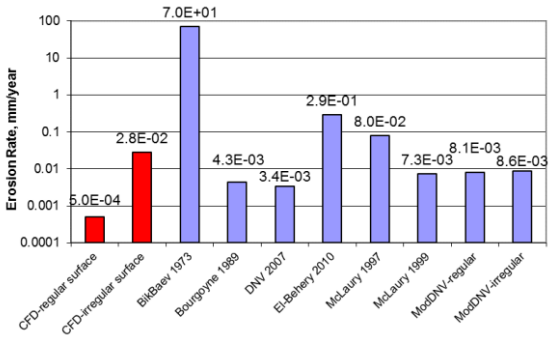

Figure 10: Comparison of modified DNV with CFD results on the 6" flexible pipe simulation.

CONCLUSIONS

The literature study has found that there very few methodologies that predict erosion by sand particles in bent pipes with smooth bores. Prediction among these models with a selected range of actual experimental data suggests that none of them can predict each set of experimental data consistently within ±50%. Most of the models generally predict the selected experimental data within one order of magnitude at best.

An attempt was made to develop a new methodology to predict the erosion rate on rough bore flexible pipe. The proposed methodology is based on the DNV-RP-O501 model. CFD flow and erosion simulations of a 6" flexible pipe steel carcass revealed that the erosion distribution around a corrugated carcass detail

qualitatively compares well with hand calculations where erosion on the curved forward-facing side of the carcass geometry is consistently higher than the smooth carcass walls.

ACKNOWLEDGEMENTS

The authors acknowledge Technip for funding this work. The authors also thank CSIRO, Technip and conference peer-reviewers for their constructive and thoughtful comments.

REFERENCES

ANSYS, (2012), "ANSYS-CFX 14.0 User Manual". Canonsburg, PA, USA, ANSYS Inc.

BIKBAEV, F.A., MAKSIMENKO, M.Z., BEREZIN, V.L., ZHILINKSI, I.B. and OTROSHKO, N.T., (1973), "Main factors affecting gas abrasive wear of elbows in pneumatic conveying pipes. ", Khimicheskoe I Neftyanoe Mashinostroenie **1**, 35-36.

BOURGOYNE, A.T., (1989), "Experimental study of erosion in diverter systems due to sand production". SPE/IADC Drilling conference, New Orleans, Louisiana, 28 Feb – 3 Mar.

DNV, (2007), "Recommended Practice RPO501 Erosive Wear in Piping Systems Rev 4.2".

EL-BEHERY, S.M., HAMED, M.H., IBRAHIM, K.A. and EL-KADI, M.A., (2010), "CFD evaluation of solid particles erosion in curved ducts", J .Fluids Engng **132**, 071303-071301-071310.

ELFEKI, S. and TABAKOFF, W., (1987), "Erosion Study of Radial Flow Compressor with Splitters", Journal of Turbomachinery-Transactions of the Asme **109**(1), 62-69.

FINNIE, I., (1960), "Erosion of Surfaces by Solid Particles", Wear **3**(2), 87-103.

JORDAN, K., (1998), "Erosion in Multiphase Production of Oil and Gas". Corrosion 98, San Diego, Ca. NACE International.

KVERNVOLD, O. and NOKLEBERG, L., (1989), "FPS2000/Flexible pipes - Erosion in flexible pipes". **Veritec 89-3303**.

KVERNVOLD, O., SANDBERG, R., RONOLD, A. , (1990), "Experimental investigation of the erosion characteristics of the steel carcass in COFLEXIP flexible pipes. 2" Rough Bore flexible pipe, gas phase only.". **Veritec Report No. 90-3691**.

MCLAURY, B.S., SHIRAZI, S.A., SHADLEY, J.R. and RYBICKI, E.F., (1999), "How Operating and Environmental Conditions Affect Erosion". Corrosion 99. NACE International.

MCLAURY, B.S., WANG, J., SHIRAZI, S.A., SHADLEY, J.R. and RYBICKI, E.F., (1997), "Solid Particle Erosion in Long Radius Elbows and Straight Pipes". SPE Annual Technical Conference and Exhibition, San Antonio, Texas, 5-8 Oct.

MENGUTURK, M. and SVERDRUP, E.F., 1979-- Calculated tolerance of a large utility gas turbine to erosion damage by coal ash particles. . Erosion: Prevention and Useful Applications, ASTM STP 664. W. F. Adler, ASTM: 193-224.

O'FLYNN, D.J., BINGLEY, M.S., BRADLEY, M.S.A. and BURNETT, A.J., (2001), "A model to predict the solid particle erosion rate of metals and its assessment using heat-treated steels", Wear **248**(1–2), 162-177.

RUFF, A.W., (1986), "Analysis of interlaboratory test results of solid particle impingement erosion", Wear **108**(4), 323-335.

SHIRAZI, S.A., MCLAURY, B.S., SHADLEY, J.R. and RYBICKI, E.F., (1995), "Generalization of the API RP 14E Guideline for Erosive Services", J. Pet. Tech, 693-698.

SUNDARARAJAN, G., (1983), "An analysis of the localization of deformation and weight loss during single-particle normal impact", Wear **84**(2), 217-235.

SUNDARARAJAN, G., (1991), "The depth of plastic deformation beneath eroded surfaces: The influence of impact angle and velocity, particle shape and material properties", Wear **149**(1–2), 129-153.

SUNDARARAJAN, G., (1995), "The solid particle erosion of metallic materials: The rationalization of the influence of material variables", Wear **186–187, Part 1**(0), 129-144.

TOGERSEN, T.G., LEJON, K., KVERNVOLD, O. and TOBERGSEN, L.E., (2006), "SNORRE A sand production management experience and solutions.", TUV NEL Sand production management seminar.

